GSA DATA REPOSITORY

SUPPLEMENTARY METHODS

Experimental design

$CaCO_3$ nucleation in the presence of PO_4 was examined with two types of experiments (Fig. DR1) conducted in synthetic Tonian composition seawater (Table DR1) that was based on fluid inclusion constraints; Spear et al., (2014) as described in the main text). $CaCO_3$ nucleation was first examined with *degassing* experiments (Fig. DR1) where CO_2 was degassed to increase the $CaCO_3$ supersaturation (Ω_{Cal}) until nucleation occurs based on He and Morse, (1993) and Lee and Morse, (2010) as described in the main text. Continuous monitoring of pH, in combination with known [Ca^{2+}] and total alkalinity (TA), constrained the carbonate chemistry at the point of nucleation (Table DR1). $CaCO_3$ nucleation was also examined with *constant composition* experiments (Fig. DR1) based on Beck et al., (2013), where the desired Ω_{Cal}, dissolved inorganic carbon (DIC), ionic strength, and TA were maintained via autotitration as described the main text. Continuous monitoring of pH and [Ca^{2+}], with ion selective and AgCl reference electrodes, constrained carbonate chemistry at the point of nucleation as described the main text.

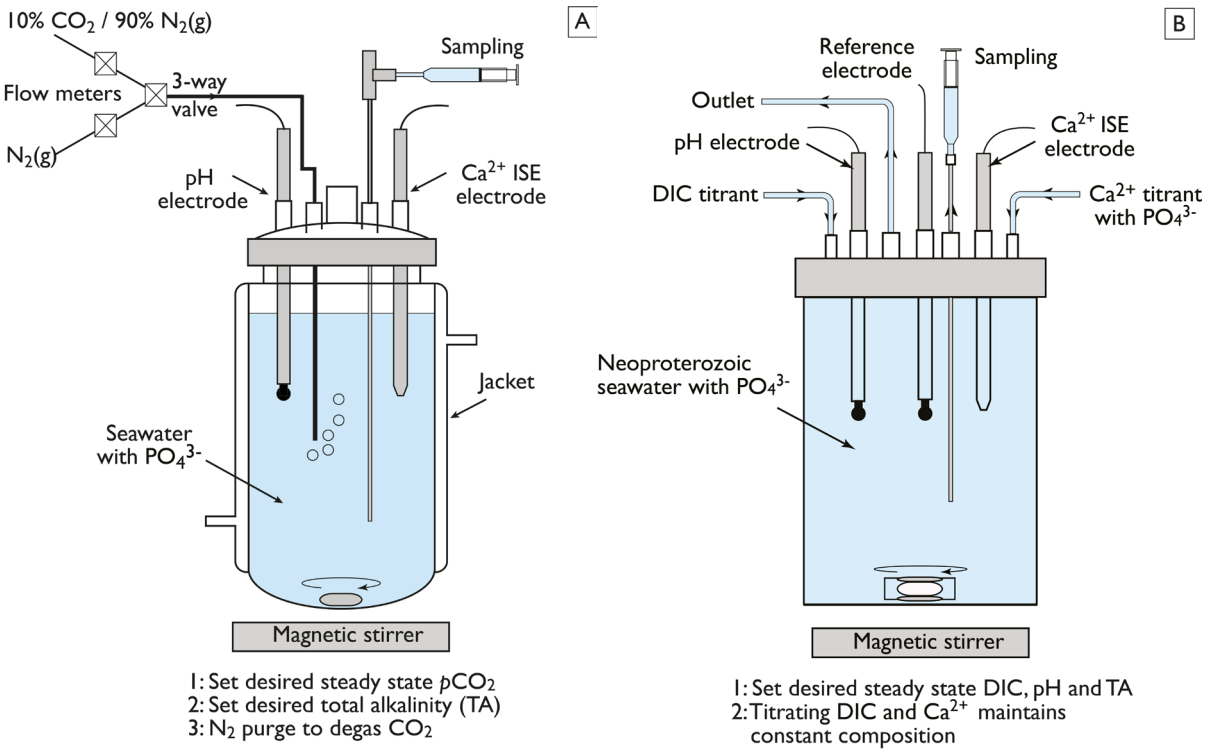

Figure DR1. Schematic diagram of A: *degassing experiment* set up indicating the CO_2 and N_2 gas inlet and measurement electrodes and B: *constant composition experiment* set up indicating the DIC and Ca^{2+} titrant inlets and measurement electrodes as described in the main text. Arrows indicate direction of flow.

Bulk PO_4 method

During constant composition experiments, solution samples (1.5 mL) were syringe-filtered (0.22 μm) and acidified (6 mL HNO_3, 4 %) for solution sample total PO_4 concentration ([PO_{4tot})], determined by spectrophotometry using the ascorbic acid method (PhosVer3 Ascorbic Acid Method 8048, Hach Lange) that determines the PO_4 concentration by detecting the absorbance at a wavelength of 680nm of the reduced phosphate-molybdate complex in solution (Baird et al., 2017).

Experiment solution chemistry

Table DR1.A

EXP ID	pH	DIC molal	Ω_{cal}	Mg^{2+}/Ca^{2+}	CO_3^{2-}/Ca^{2+}	TA molal	Ionic strength molal
1-A 310718	9.2	0.025	301	5.56	1.59	0.039	0.67
1-B 101018R	8.8	0.025	183	5.56	0.96	0.034	0.65
1-C 210818	8.3	0.025	75	5.56	0.40	0.028	0.66
1-D 170918	7.7	0.025	21	5.56	0.11	0.026	0.65
1-E 241018R	9.2	0.015	181	5.56	0.95	0.024	0.66
1-F 301018	8.8	0.015	110	5.56	0.58	0.020	0.65
1-G 061110	8.3	0.015	45	5.56	0.24	0.017	0.65
2-MB 300419	8.7	0.010	83	3.33	0.25	0.013	0.63
2-MBR 040619	8.7	0.010	83	3.33	0.25	0.013	0.63
2-MCR 170619	8.7	0.010	83	3.33	0.25	0.013	0.63
2-SI 290719	8.5	0.014	83	3.33	0.25	0.013	0.63
2-EB 100419	8.1	0.024	60	3.33	0.18	0.026	0.64
2-F 211118	9.2	0.014	169	5.56	0.89	0.022	0.66
2-H 240119	8.7	0.014	117	3.33	0.35	0.018	0.64
2-I 140119	8.5	0.014	83	3.33	0.25	0.013	0.63
2-I-R 170118	8.5	0.014	83	3.33	0.25	0.013	0.63
2-J 280119	8.3	0.014	56	3.33	0.17	0.016	0.63
2-MR 190219	8.7	0.010	83	3.33	0.25	0.013	0.63
2-N 270219	8.5	0.010	59	3.33	0.17	0.012	0.63
2-Q 050319	8.9	0.025	113	3.33	0.33	0.014	0.63
2-X 270220	8.7	0.014	117	2.86	0.21	0.013	0.63

33

Table DR1.B

EXP ID	[Na] molal	[K] molal	[Mg] molal	[Ca] molal	[Si] molal	[SO_4] molal	[Cl] molal	[PO_4] umolal	[HCO_3] molal	[CO_3] molal	[CO_2]
1-A 310718	0.452	0.010	0.050	0.009	0.00	0.003	0.565	50	0.0107	0.0143	0.00001
1-B 101018R	0.452	0.010	0.050	0.009	0.00	0.003	0.565	50	0.0163	0.0087	0.00003
1-C 210818	0.452	0.010	0.050	0.009	0.00	0.003	0.565	50	0.0213	0.0036	0.00011
1-D 170918	0.452	0.010	0.050	0.009	0.00	0.003	0.565	50	0.0235	0.0010	0.00048
1-E 241018R	0.452	0.010	0.050	0.009	0.00	0.003	0.565	50	0.0064	0.0086	0.00000
1-F 301018	0.452	0.010	0.050	0.009	0.00	0.003	0.565	50	0.0098	0.0052	0.00002
1-G 061110	0.452	0.010	0.050	0.009	0.00	0.003	0.565	50	0.0128	0.0022	0.00006
2-MB 300419	0.452	0.010	0.040	0.012	0.00	0.003	0.565	100	0.0070	0.0030	0.00001
2-MBR 040619	0.452	0.010	0.040	0.012	0.00	0.003	0.565	100	0.0070	0.0030	0.00001
2-MCR 170619	0.452	0.010	0.040	0.012	0.00	0.003	0.565	25	0.0070	0.0030	0.00001
2-SI 290719	0.452	0.010	0.040	0.012	0.00	0.003	0.565	50	0.0070	0.0030	0.00001
2-EB 100419	0.452	0.010	0.040	0.012	0.00	0.003	0.565	50	0.0217	0.0021	0.0002
2-F 211118	0.452	0.010	0.050	0.009	0.00	0.003	0.565	50	0.0060	0.0080	0.0000
2-H 240119	0.452	0.010	0.040	0.012	0.00	0.003	0.565	50	0.0098	0.0042	0.0000
2-I 140119	0.452	0.010	0.040	0.012	0.00	0.003	0.565	50	0.0070	0.0030	0.00001
2-I-R 170118	0.452	0.010	0.040	0.012	0.00	0.003	0.565	50	0.0070	0.0030	0.00001
2-J 280119	0.452	0.010	0.040	0.012	0.00	0.003	0.565	50	0.0119	0.0020	0.0001
2-MR 190219	0.452	0.010	0.040	0.012	0.00	0.003	0.565	50	0.0070	0.0030	0.0000
2-N 270219	0.452	0.010	0.040	0.012	0.00	0.003	0.565	50	0.0079	0.0021	0.0000
2-Q 050319	0.452	0.010	0.040	0.012	0.00	0.003	0.565	50	0.0060	0.0040	0.0000
2-X 270420	0.452	0.010	0.040	0.014	0.00	0.003	0.565	50	0.0070	0.0030	0.0000

Note: HCO_3, CO_3 and CO_2 were computed using relationships and constants in Zeebe and Wolf-Gladrow (2001).

34

35

Table DR1.C

EXP ID	pH	DIC molal	Ω_{cal}	Mg^{2+}/Ca^{2+}	CO_3^{2-}/Ca^{2+}	TA molal
110716	8.56	0.0115	21.37	5.55	0.300	0.0142
130716	8.70	0.0039	25.83	5.55	0.165	0.0054
140716	8.86	0.0028	22.42	5.55	0.119	0.0039
190716	7.63	0.0229	17.65	5.55	0.228	0.0248
250716	9.21	0.0076	92.69	5.55	0.490	0.0120
260916	8.87	0.0145	117.33	5.55	0.620	0.0201
101016	8.51	0.0265	118.97	5.55	0.629	0.0320
311017	8.76	0.0215	147.62	5.55	0.780	0.0285
021117	8.60	0.0218	114.89	5.55	0.608	0.0272
061117	8.48	0.0232	98.79	5.55	0.522	0.0278
241016	8.87	0.0087	117.40	2.67	0.223	0.0120
191016	8.33	0.0156	83.10	2.67	0.158	0.0179
171016	8.42	0.0236	150.11	2.67	0.285	0.0278
131117	8.64	0.0196	184.29	2.67	0.350	0.0248
141117	8.64	0.0196	184.29	2.67	0.350	0.0248

36

37

Table DR1.D

EXP ID	[Ca] molal	[Mg] molal	KH_2PO_4 umolal	SiO_2 molal	pCO_2 uatm	$[CO_3^{2-}]$ molal
110716	0.0090	0.0499	0	0.0017	866	0.0027
130716	0.0090	0.0499	0	0.0017	120	0.0015
140716	0.0090	0.0499	0	0.0017	86	0.0011
190716	0.0090	0.0499	0	0.0017	6282	0.0020
250716	0.0090	0.0499	50	0.0017	71	0.0044
260916	0.0090	0.0499	50	0.0017	430	0.0056
101016	0.0090	0.0499	50	0.0017	2286	0.0057
311017	0.0090	0.0499	23	0.0017	897	0.0070
021117	0.0090	0.0499	12	0.0017	1459	0.0055
061117	0.0090	0.0499	6	0.0017	2180	0.0047
241016	0.0150	0.0400	50	0.0017	258	0.0033
191016	0.0150	0.0400	50	0.0017	2192	0.0024
171016	0.0150	0.0400	50	0.0017	2617	0.0043
131117	0.0150	0.0400	75	0.0017	1167	0.0053
141117	0.0150	0.0400	100	0.0017	1167	0.0053

38

39 **Table DR1.** Details of carbonate chemistry at the point of nucleation. A: constant composition
40 experimental parameters. B: constant composition solution chemistry. C: degassing experimental
41 parameters. D: degassing solution chemistry. HCO_3, CO_3 and CO_2 were computed using
42 relationships and constants in Zeebe and Wolf-Gladrow, (2001). Mg/Ca and CO_3/Ca are molar
43 ratios.

44

45

SOLID SAMPLE CHARACTERISATION

Rietveld refinement

The Mg content of the solids was estimated by Rietveld refinement (Table DR 2A) using GSAS-II (Larson and Von Dreele, 2004) with structural models for Mg-calcite reported in Paquette and Reeder (1990) and calibrations determined by Titschack et al. (2011). X-ray diffraction patterns (XRD) (Fig. DR2) represent amorphous calcium magnesium carbonate (ACMC) and resultant solids.

Table DR2.A

			Calcite				
EXP ID	Phases	Residual wR	wt. %	a (Å)	c (Å)	volume (Å^3)	Estimated Mg content (mol %)
2Q-050319	Mg-calcite + MHC	4.198%	75.0	4.97789	16.96770	364.120	3.34
2I-140219	Mg-calcite	9.666%	100.0	4.97614	16.98467	364.228	3.23
2M-190219	Mg-calcite + MHC	4.259%	87.5	4.96822	16.93305	361.966	5.65
1C-210818	Mg-calcite	5.935%	100.0	4.97335	16.97488	363.610	3.89
2I-140119	Mg-calcite	8.354%	100.0	4.97634	16.99683	364.517	2.92
A-171016	Mg-calcite + MHC	5.014%	96.8	4.96725	16.95286	362.247	5.35
A-141117	Mg-calcite + MHC + arag	9.55%	86.0	4.96884	16.95949	362.621	4.95
A-241016	Mg-calcite + MHC	13.10%	77.5	4.94545	16.87389	357.402	10.5

Table DR2.B

		Monohydrocalcite			
EXP ID	Phases	wt. %	a (Å)	c (Å)	volume (Å^3)
2Q-050319	Mg-calcite + MHC	25.0	10.59414	7.53753	732.642
2I-140219	Mg-calcite	--	--	--	--
2M-190219	Mg-calcite + MHC	12.5	10.58886	7.52948	731.128
1C-210818	Mg-calcite	--	--	--	--
2I-140119	Mg-calcite	--	--	--	--
A-171016	Mg-calcite + MHC	3.2	10.57972	7.54315	731.192
A-141117	Mg-calcite + MHC + arag	2.7	10.52771	7.41047	711.286
A-241016	Mg-calcite + MHC	22.5	10.56369	7.47366	722.263

Table DR2. Rietveld refinement of synthetic samples produced from experiments that contain Mg-calcite, monohydrocalcite (MHC) and aragonite (arag). A: Rietveld refinement values for Mg-calcite. B: Rietveld refinement values for monohydrocalcite.

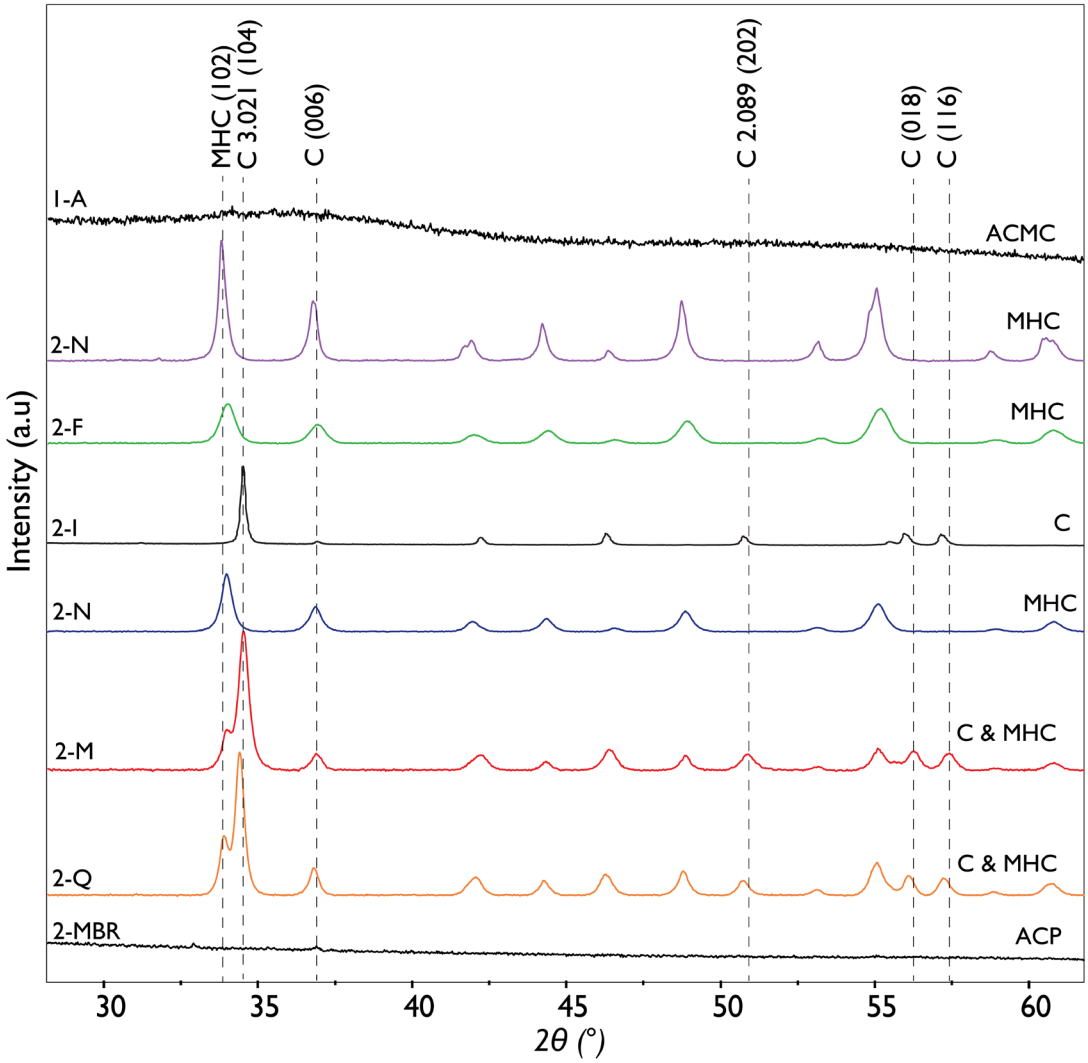

Figure DR2. XRD solid sample characterization from experimental solutions with Bragg peaks assigned. Amorphous-Ca-Mg-carbonate (ACMC), monohydrocalcite (MHC), calcite (C) and amorphous calcium phosphate (ACP).

Spectroscopy

Ex-situ FT-IR analyses display diagnostic absorbance features in vibrational spectroscopy (Fig. DR3). Amorphous calcium phosphate (ACP) also nucleates in experiments where PO_{4tot} approached 100 μmolal (along with ACMC), which recrystallized to octocalcium phosphate (OCP) over 48 hours (Fig. DR3). FTIR spectra also indicate that poorly crystalline calcium phosphate phases may be present and associated with samples containing monohydrocalcite and calcite (Fig. DR3).

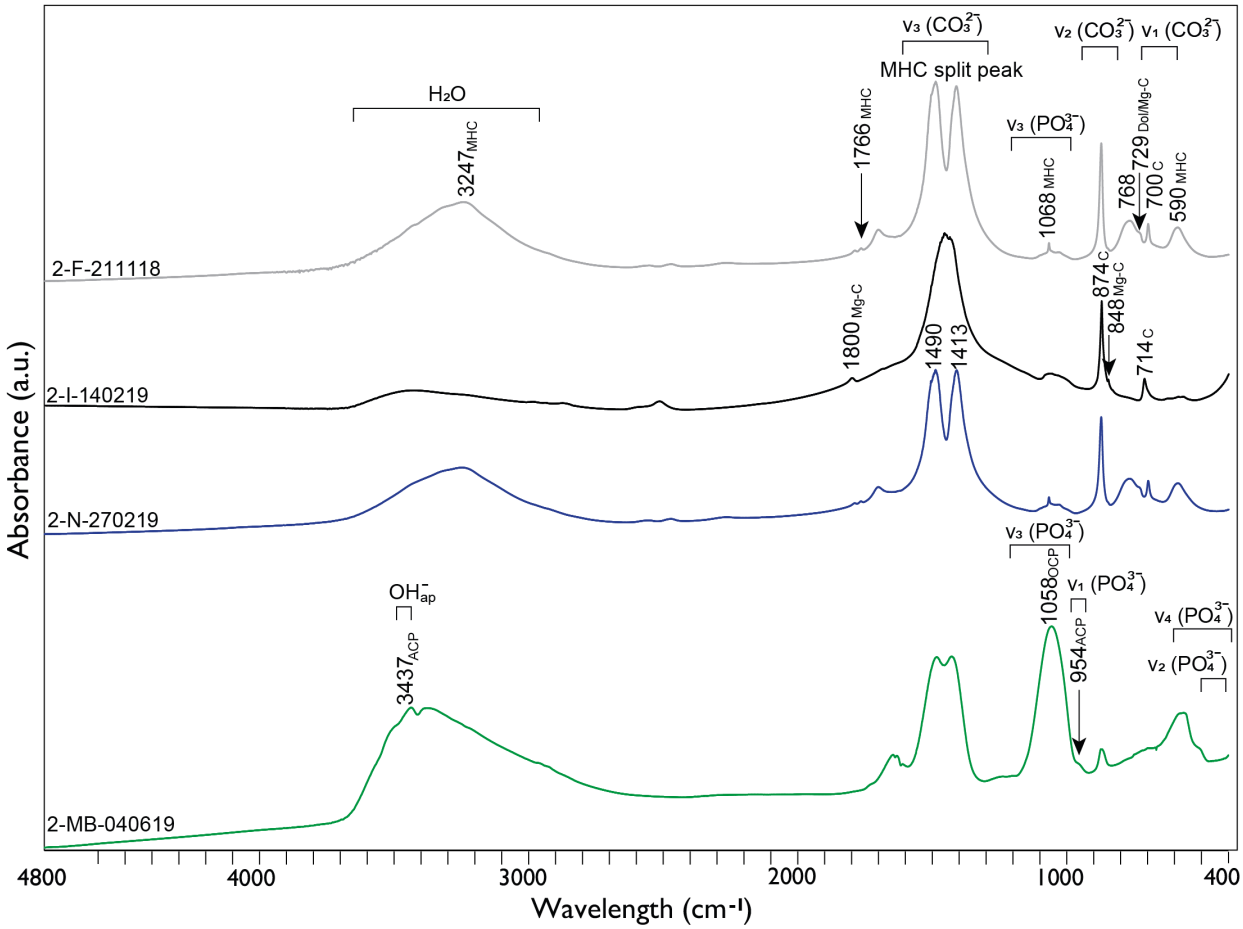

Figure DR3. FTIR sample characterization of monohydrocalcite (MHC), calcite (C) and octacalcium phosphate (OCP) with peaks representing apatite (ap) and amorphous calcium phosphate (ACP) also labelled.

REFERENCES CITED

Baird, R., Eaton, A.D., Andrew, D., Rice, E.W. and Bridgewater, L., 2017, Standard methods for the examination of water and wastewater: American Public Health Association. v. 23, p. 4500, https://doi.org/10.2105/SMWW.2882.093.

Beck, R., Seiersten, M., and Andreassen, J.P., 2013, The constant composition method for crystallization of calcium carbonate at constant supersaturation: Journal of Crystal Growth, v. 380, p. 187–196, https://doi.org/10.1016/j.jcrysgro.2013.05.038.

He, S., and Morse, J.W., 1993, The carbonic acid system and calcite solubility in aqueous Na-K-Ca-Mg-Cl-SO_4 solutions from 0 to 90°C: Geochimica et Cosmochimica Acta, v. 57(15), p. 3533-3554, https://doi.org/10.1016/0016-7037(93)90137-L.

Larson, A.C., and Von Dreele, R.B., 2004, General Structure Analysis System (GSAS): Los Alamos National Laboratory Report-LAUR, p. 86-748, https://doi.org/10.1103/PhysRevLett.101.107006.

Lee, J., and Morse, J.W., 2010, Influences of alkalinity and pCO2 on CaCO3 nucleation from estimated Cretaceous composition seawater representative of "calcite seas": Geology, v. 38, p. 115–118, https://doi.org/10.1130/G30537.1.

Paquette, J., Reeder, R.J., 1990, Single-crystal X-ray structure refinements of two biogenic magnesian calcite crystals: American Mineralogist, v. 75(9-10), p. 1151–1158.

Spear, N., Holland, H.D., Garcia-Veígas, J., Lowenstein, T.K., Giegengack, R., and Peters, H., 2014, Analyses of fluid inclusions in Neoproterozoic marine halite provide oldest measurement of seawater chemistry: Geology, v. 42, p. 103–106, https://doi.org/10.1130/G34913.1.

Titschack, J., Goetz-Neunhoeffer F. and Neubauer J. (2011) Magnesium quantifcation in calcites [(Ca, Mg)CO_3] by Rietveld-based XRD analysis: Revisiting a well-established method. Am. Mineral. v. 96, p. 1028–1038, https://doi.org/10.2138/am.2011.3665.

Zeebe, R.E., and Wolf-Gladrow, D., 2001, CO_2 in Seawater: Equilibrium, Kinetics, Isotopes: Amsterdam, Elsevier Science, v. 65. 360 p.